

# MOTT–HUBBARD LOCALIZATION IN A MODEL OF THE ELECTRONIC SUBSYSTEM OF DOPED FULLERIDES

YU. DOVHOPYATY,<sup>1</sup> L. DIDUKH,<sup>1</sup> O. KRAMAR,<sup>1</sup> YU. SKORENKYY,<sup>1</sup>  
YU. DROHOBITSKY<sup>2</sup>

<sup>1</sup>Ternopil National Technical University

(56, Ruska Str., Ternopil 46001, Ukraine; e-mail: didukh@tu.edu.te.ua)

<sup>2</sup>Ternopil National Pedagogical University

(2, M. Kryvonosa Str., Ternopil 46027, Ukraine)

UDC 537.312.62, 538.945  
© 2012

A microscopical model of doped fulleride electronic subsystem taking the triple orbital degeneracy of energy states into account is considered within the configurational-operator approach. Using the Green function method, the energy spectrum at the integer band filling  $n = 1$  corresponding to  $AC_{60}$  compounds is calculated. A possible correlation-driven metal-insulator transition within the model is discussed.

## 1. Introduction

Electrical, optical, and mechanical properties of fullerenes [1, 2] in the condensed state demonstrate a considerable physical content of phenomena, which take place in fullerenes, and show that the use of such materials in electronics has significant perspectives. Fullerene crystals and films are semiconductors with an energy gap of 1.2–1.9 eV [3, 4] and have photoconductivity under visible light irradiation. Fullerene crystals have comparatively small binding energy, and the phase transition connected with the orientational disordering of fullerene molecules occurs in such crystals at room temperature [5].

The addition of radicals containing platinum-group metals [6] to fullerenes  $C_{60}$  allows one to obtain ferromagnetic materials based on fullerene. In polycrystal  $C_{60}$  doped by an alkali metal, the superconductivity at temperatures lower than 33 K is observed [7, 8]. The large binding energy is typical of metallocarbohedra  $M_8C_{12}$ , where  $M = Ti, V, Hg, Zr$ . For example, in  $Ti_8C_{12}$ , the molecule binding energy per atom is 6.1 eV [9] (for a  $C_{60}$  molecule, this energy is 7.4–7.6 eV [3]).

Fullerenes in the solid state (fullerites) are molecular crystals, where the interaction between atoms in  $C_{60}$  molecule is much larger than the interaction between nearest molecules. In a closely packed structure, each fullerene molecule has 12 nearest neighbors. Depending

on peculiarities of the molecular interaction, the face-centered cubic lattice or hexagonal lattice is realized [10]. A phase transition in the  $C_{60}$  crystal occurs at a temperature of 257 K, and this is the first-order transition. At high temperatures, molecules can freely rotate, whereas the rotation at low temperatures is stopped, and the interaction anisotropy of neighbor molecules  $C_{60}$  becomes important. This leads to a small sharp change of the distance between the nearest molecules. According to the results of X-ray structure analysis [11], the lattice constant changes from  $1.4154 \pm 0.0003$  nm to  $1.4111 \pm 0.0003$  nm (that is, by  $0.43 \pm 0.06$  percent).

At low temperatures, when  $C_{60}$ -molecules are oriented in space, the crystal lattice symmetry does not coincide with the symmetry of a single molecule  $C_{60}$  (icosahedral symmetry  $Y$ ). In a unit cell of the fullerite crystal lattice, there are four  $C_{60}$ -molecules. These molecules form a tetrahedron, in which orientations of all molecules are the same. Tetrahedra, in turn, form a simple cubic lattice.

Fullerites are semiconductors with an energy gap of 1.5–1.95 eV [3]. The electrical resistivity of polycrystals  $C_{60}$  [11] monotonically changes with the temperature, and the energy gap has monotonic dependence on the pressure: an increase of the energy gap under the pressure higher than  $2 \times 10^5$  atm indicates the absence of the metal-insulator transition at  $p \simeq 10^6$  atm. In the temperature region 150–400 K, the relaxation time is temperature-independent, which indicates that the carriers are localized, and the hopping mechanism of recombination, which includes the tunneling of electrons between localized states, is realized.

It has been shown in [7] that the doping of solid fullerenes  $C_{60}$  by a small amount of an alkali metal leads to the formation of a material with the metallic type of conductivity, and this material becomes superconducting at low temperatures ( $T_c$  from 2.5 K for  $Na_2KC_{60}$

to 33 K for  $\text{RbCs}_2\text{C}_{60}$ ). At changes of the temperature, concentration of an alkali metal, and parameters and structure of the lattice, various phases of these compounds have been realized. In particular, at various fillings  $n$  ( $n$  may change from 0 to 6) of the lowest unoccupied molecular orbital (LUMO), the metallic, insulating, or superconducting phases have been realized. Superconductivity in doped fullerenes  $\text{K}_x\text{C}_{60}$  has been studied theoretically in [12], and strong electron correlations have been shown to play a crucial role in the superconducting state stabilization. Recently, the strong electron correlation was also proven [13] to be responsible for the superconductivity of planar carbon systems of the graphene type.

Let us consider the electronic structure of  $\text{C}_{60}$  in detail. In the single-particle approximation with neglect of electron correlations, the following spectrum has been calculated [2]: 50 of 60  $p_z$  electrons of a neutral molecule fill all orbitals up to  $L = 4$ . The lowest  $L = 0, 1, 2$  orbitals correspond to icosahedral states  $a_g, t_{1u}, h_g$ . All states with greater  $L$  undergo the icosahedral-field splitting. There are 10 electrons in the partially filled  $L = 5$  state. The icosahedral splitting ( $L = 5 \rightarrow h_u + t_{1u} + t_{2u}$ ) of this 11-fold degenerate orbital leads to the electronic configuration shown below. Microscopic calculations and experimental data show that the completely filled highest occupied molecular orbital is of  $h_u$  symmetry, and LUMO (3-fold degenerate) has  $t_{1u}$  symmetry. Under such conditions, the HOMO-LUMO gap appears due to the icosahedral perturbation in the shell with  $L = 5$ ; the energy gap found experimentally is about 1 eV for molecules in vacuum. The  $t_{2g}$  (LUMO+1)-state originated from  $L = 6$  shell is found approximately to be 1 eV above the  $t_{1u}$  LUMO.

Electron-electron correlations in  $\text{C}_{60}$  are described by two main parameters: the intramolecular Coulomb repulsion  $U$  and Hund's coupling  $J_H$ . In fullerenes, the competition between the intrasite Coulomb interaction (Hubbard  $U$ ) and delocalization processes related to the translational motion of electrons (which determines the bandwidth) causes the realization of the insulator or metallic state [14]. The majority of experimental data and theoretical calculations indicate that all materials with ions  $\text{C}_{60}^{-n}$  at integer  $n$  are Mott-Hubbard insulators, as  $U$  is quite large for all doped compounds  $\text{A}_x\text{C}_{60}$ . Fullerenes  $\text{A}_x\text{C}_{60}$  doped with alkali metals  $\text{A}$  attract much attention of researchers due to the unusual metal-insulator transition in these compounds. Only  $\text{A}_3\text{C}_{60}$  is metallic, and other phases  $\text{AC}_{60}$ ,  $\text{A}_2\text{C}_{60}$  and  $\text{A}_4\text{C}_{60}$  are insulator ones [15]. This experimental fact contradicts the results of band structure calculations (see,

e.g., [16]), which predict the purely metallic behavior. It has been noted in [17] that, to explain the metallic behavior of the Mott-Hubbard system ( $x = 3$  corresponds to the half-filling of the conduction band), one has to consider a degeneracy of the energy band. On the base of the Gutzwiller variational approach, the metal-insulator transition has been proven [17] to exist for all integer band fillings. It is shown that the critical value of Coulomb interaction parameter depends essentially on the band filling and the degeneracy (in the case of half filling,  $\frac{U_c}{2w} \simeq 2.8$  for double degeneracy,  $\frac{U_c}{2w} \simeq 3.9$  for triple degeneracy). The present study is devoted to the investigation of the Mott-Hubbard localization in the electronic subsystem of fullerenes with strong electron correlations within the model involving the orbital degeneracy of energy levels, strong Coulomb interaction, and correlated hopping of electrons.

## 2. Hamiltonian of the Doped Fullerene Electronic Subsystem

Within the second quantization formalism, the Hamiltonian of interacting electron systems can be written [18] as

$$H = -\mu \sum_{i\lambda\sigma} a_{i\lambda\sigma}^+ a_{i\lambda\sigma} + \sum'_{ij\lambda\sigma} t_{ij} a_{i\lambda\sigma}^+ a_{j\lambda\sigma} + \frac{1}{2} \sum_{ijkl} \sum_{\alpha\beta\gamma\delta\sigma\sigma'} J_{ijkl}^{\alpha\beta\gamma\delta} a_{i\alpha\sigma}^+ a_{j\beta\sigma'}^+ a_{l\delta\sigma'} a_{k\gamma\sigma}, \quad (1)$$

where the first sum with the matrix element

$$t_{ij} = \int d^3r \phi_{\lambda i}^*(\mathbf{r} - \mathbf{R}_i) \times \left[ -\frac{\hbar^2}{2m} \Delta + V^{\text{ion}}(\mathbf{r}) \right] \phi_{\lambda i}(\mathbf{r} - \mathbf{R}_j) \quad (2)$$

describes the translational motion (hopping) of electrons in the crystal field  $V^{\text{ion}}(\mathbf{r})$ , and the second sum is the general expression for pair electron interactions described by the matrix elements

$$J_{ijkl}^{\alpha\beta\gamma\delta} = \int \int \phi_{\alpha}^*(\mathbf{r} - \mathbf{R}_i) \phi_{\beta}(\mathbf{r} - \mathbf{R}_j) \times \frac{e^2}{|\mathbf{r} - \mathbf{r}'|} \phi_{\delta}^*(\mathbf{r} - \mathbf{R}_l) \phi_{\gamma}(\mathbf{r} - \mathbf{R}_k) d\mathbf{r} d\mathbf{r}'. \quad (3)$$

In the above formulae,  $a_{i\lambda\sigma}^+$ ,  $a_{i\lambda\sigma}$  are the operators of spin- $\sigma$  electron creation and annihilation in the orbital

state  $\lambda$  on the lattice site  $i$ , respectively, the indices  $\alpha, \beta, \gamma, \delta$ , and  $\lambda$  denote orbital states,  $\phi_{\lambda i}$  is the wave-function in the Wannier (site) representation, other notation is standard. Hamiltonian (1) is essentially non-diagonal and hard to be treated mathematically. The problem can be greatly simplified by neglecting the matrix elements of the interaction of the third and further orders of magnitude and restricting oneself to the consideration of a single orbital per site. In this way, the Hamiltonian of the Hubbard model and many other backbone models of the theory of strongly correlated electrons were derived. However, it has been shown that these models lack the possibility to describe the electron-hole asymmetry observed in real correlated electron systems. To maintain such a possibility, we are to consider the structure of energy levels and to estimate interaction parameters prior to make simplifications. Following works [19, 20], we derive the Hamiltonian which includes the correlated hopping of electrons (the site-occupation dependence of hopping parameters results from taking the interactions with second-order matrix elements into account) and a variety of intrasite interactions caused by the triple orbital degeneracy of LUMO in doped fullerenes. The zero-order interaction integral includes the on-site Coulomb correlation (characterized by the Hubbard parameter  $U$ ):

$$U = \int \int |\phi_{\lambda}^*(\mathbf{r} - \mathbf{R}_i)|^2 \frac{e^2}{|\mathbf{r} - \mathbf{r}'|} |\phi_{\lambda}(\mathbf{r}' - \mathbf{R}_i)|^2 d\mathbf{r} d\mathbf{r}'. \quad (4)$$

In an orbitally degenerate system, the on-site (Hund's rule) exchange integral

$$J_H = \int \int \phi_{\lambda}^*(\mathbf{r} - \mathbf{R}_i) \phi_{\lambda'}(\mathbf{r} - \mathbf{R}_i) \frac{e^2}{|\mathbf{r} - \mathbf{r}'|} \times \phi_{\lambda'}^*(\mathbf{r}' - \mathbf{R}_i) \phi_{\lambda}(\mathbf{r}' - \mathbf{R}_i) d\mathbf{r} d\mathbf{r}', \quad (5)$$

is of principal importance as well. The parameter  $U$  for fullerenes had been estimated within different methods. The local density approximation (LDA) gives 3.0 eV [21, 22]. Experimental estimation of the electron repulsion energy [23] gives  $U \simeq 2.7$  eV.

It is worth to note that, in the solid state, molecules are placed close enough to provide a substantial screening of the interaction. The calculation with regard for the screening effect gives  $U$  2.7 eV [21, 22]. Combining Auger spectroscopy and photoemission spectroscopy lead to the value 1.4-1.6 eV [24, 25] for  $U$ . We also note that the energy cost of electron configurations with spins aligned in parallel is considerably less than that for the antiparallel alignment. Orbitally degenerate levels are filled according to Hund's rule. Experimental

methods [24] give  $0.2 \text{ eV} \pm 0.1 \text{ eV}$  for the singlet-triplet splitting; whereas its value is close to 0.05 eV according to [26]. The relevant intersite parameters are the electron hopping integral and the intersite exchange coupling  $J(i\lambda j\lambda' j\lambda i\lambda')$ .

The resulting Hamiltonian of the doped fullerene electronic subsystem reads

$$\begin{aligned} H = & -\mu \sum_{i\lambda\sigma} a_{i\lambda\sigma}^+ a_{i\lambda\sigma} + U \sum_{i\lambda} n_{i\lambda\uparrow} n_{i\lambda\downarrow} + \\ & + \frac{U'}{2} \sum_{i\lambda\sigma} n_{i\lambda\sigma} n_{i\lambda'\bar{\sigma}} + \frac{U' - J_H}{2} \sum_{i\lambda\lambda'\sigma} n_{i\lambda\sigma} n_{i\lambda'\sigma} + \\ & + \sum'_{ij\lambda\sigma} t_{ij}(n) a_{i\lambda\sigma}^+ a_{j\lambda\sigma} + \sum'_{ij\lambda\sigma} t'_{ij} (a_{i\lambda\sigma}^+ a_{j\lambda\sigma} n_{i\bar{\lambda}} + \text{h.c.}) + \\ & + \sum'_{ij\lambda\sigma} t''_{ij} (a_{i\lambda\sigma}^+ a_{j\lambda\sigma} n_{i\lambda\bar{\sigma}} + \text{h.c.}), \end{aligned} \quad (6)$$

where  $n_{i\lambda\sigma} = a_{i\lambda\sigma}^+ a_{i\lambda\sigma}$ ,  $U' = U - 2J_H$ , and the hopping integrals  $t_{ij}(n)$ ,  $t'_{ij}$ ,  $t''_{ij}$  with regard for three types of correlated hopping of electrons [28] are introduced.

In a model of triply degenerate band, every site can be in one of 64 configurations (see Fig. 1). To pass from the electron operator to the Hubbard operators  $X^{pl}$  of the transition from state  $|l\rangle$  to state  $|p\rangle$ , we use the relations

$$\begin{aligned} \hat{a}_{\alpha\uparrow}^+ = & X^{\uparrow 00,000} + X^{200,\downarrow 00} + X^{\uparrow 0,0\uparrow 0} + X^{\uparrow \downarrow 0,0\downarrow 0} + \\ & + X^{\uparrow 0\uparrow,00\uparrow} + X^{\uparrow 0\downarrow,00\downarrow} + X^{\uparrow 20,020} + X^{\uparrow 02,002} + \\ & + X^{2\downarrow 0,\downarrow\downarrow 0} + X^{20\downarrow,\downarrow 0\downarrow} + X^{\uparrow\uparrow\uparrow,0\uparrow\uparrow} + X^{\uparrow\downarrow\downarrow,0\downarrow\downarrow} + \\ & + X^{2\uparrow 0,\uparrow\uparrow 0} + X^{20\uparrow,\downarrow 0\uparrow} + X^{\uparrow\uparrow\downarrow,0\uparrow\downarrow} + X^{\uparrow\uparrow\downarrow,0\downarrow\uparrow} + \\ & + X^{2\downarrow\downarrow,\downarrow\downarrow\downarrow} + X^{2\downarrow\uparrow,\downarrow\downarrow\uparrow} + X^{2\uparrow\downarrow,\downarrow\uparrow\downarrow} + X^{2\uparrow\uparrow,\downarrow\uparrow\uparrow} + \\ & + X^{220,\downarrow 20} + X^{\uparrow 2\uparrow,02\uparrow} + X^{\uparrow 2\downarrow,02\downarrow} + X^{202,\downarrow 02} + \\ & + X^{\uparrow\uparrow 2,0\uparrow 2} + X^{\uparrow\downarrow 2,0\downarrow 2} + X^{\uparrow 22,022} + X^{22\downarrow,\downarrow 2\downarrow} + \\ & + X^{2\downarrow 2,\downarrow\downarrow 2} + X^{22\uparrow,\downarrow 2\uparrow} + X^{2\uparrow 2,\downarrow\uparrow 2} + X^{222,\downarrow 22}, \\ \hat{a}_{\alpha\downarrow}^+ = & X^{\downarrow 00,000} - X^{200,\uparrow 00} + X^{\downarrow 0,0\uparrow 0} + X^{\downarrow \downarrow 0,0\downarrow 0} + \end{aligned}$$

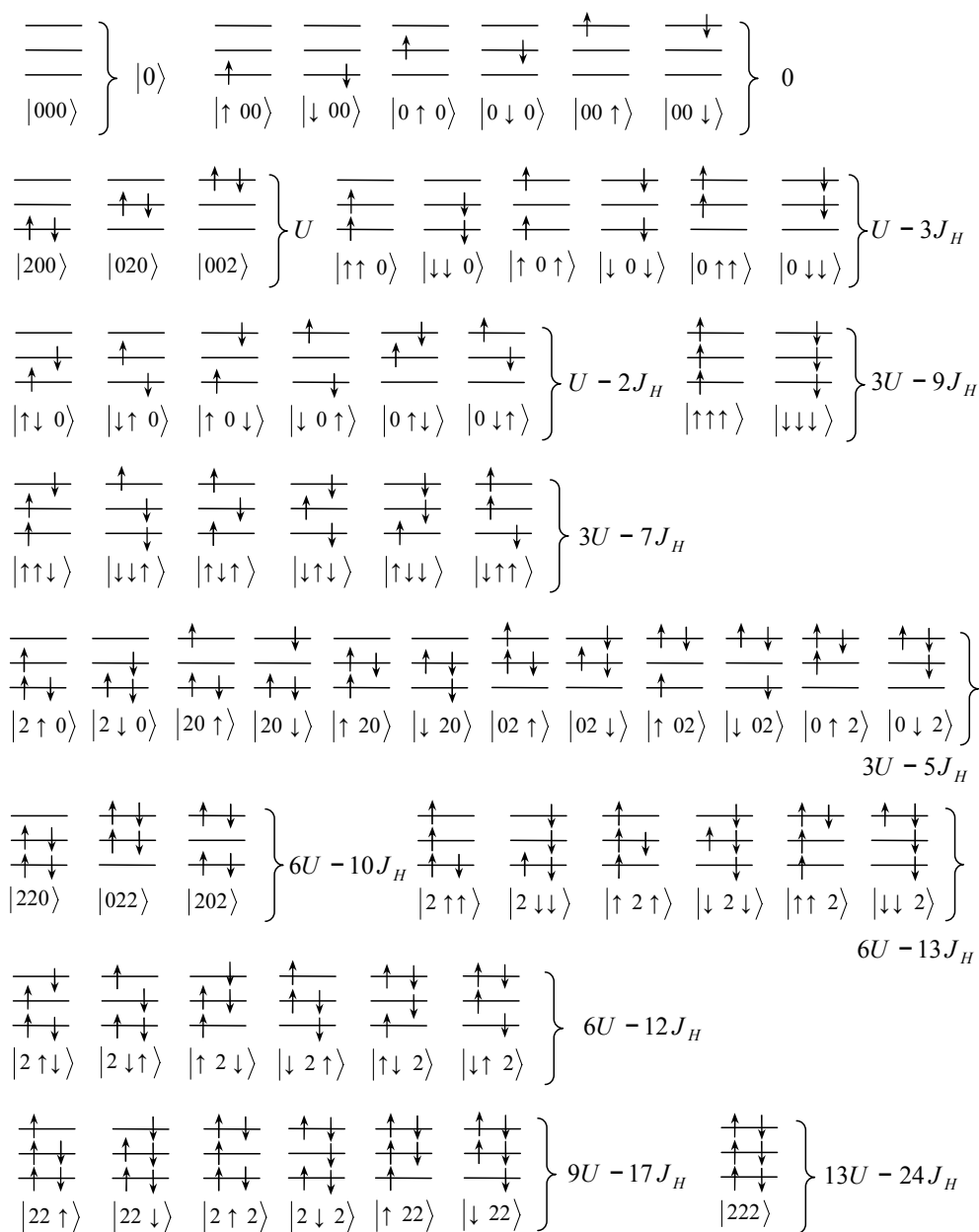


Fig. 1. Possible site configurations in the threefold degenerate model. The first symbol in the state notation corresponds to the  $\alpha$  orbital, the second and third – to the  $\beta$  and  $\gamma$  orbitals, respectively

$$\begin{aligned}
 &+X^{\downarrow 0\uparrow,00\uparrow} + X^{\downarrow 0\downarrow,00\downarrow} + X^{\downarrow 20,020} + X^{\downarrow 02,002} - \\
 &-X^{2\uparrow 0,\uparrow\uparrow 0} - X^{20\uparrow,\uparrow 0\uparrow} + X^{\downarrow\uparrow\uparrow,0\uparrow\uparrow} + X^{\downarrow\downarrow\downarrow,0\downarrow\downarrow} - \\
 &-X^{2\downarrow 0,\uparrow\downarrow 0} - X^{20\downarrow,\uparrow 0\downarrow} + X^{\downarrow\uparrow\downarrow,0\uparrow\downarrow} + X^{\downarrow\downarrow\uparrow,0\downarrow\uparrow} - \\
 &-X^{2\uparrow\uparrow,\uparrow\uparrow\uparrow} - X^{2\uparrow\downarrow,\uparrow\uparrow\downarrow} - X^{2\downarrow\uparrow,\uparrow\downarrow\uparrow} - X^{2\downarrow\downarrow,\uparrow\downarrow\downarrow} - \\
 &-X^{220,\uparrow 20} + X^{\downarrow 2\uparrow,02\uparrow} + X^{\downarrow 2\downarrow,02\downarrow} - X^{202,\uparrow 02} + \\
 &+X^{\downarrow\uparrow 2,0\uparrow 2} + X^{\downarrow\downarrow 2,0\downarrow 2} + X^{\downarrow 22,022} - X^{22\uparrow,\uparrow 2\uparrow} - \\
 &-X^{2\uparrow 2,\uparrow\uparrow 2} - X^{22\downarrow,\uparrow\downarrow 2} - X^{2\downarrow 2,\uparrow\downarrow 2} - X^{222,\uparrow 22}, \quad (7)
 \end{aligned}$$

which ensure the fulfillment of the anticommutation relations  $\{X_i^{pl}; X_j^{kt}\} = \delta_{ij}(\delta_{lk}X_i^{pt} + \delta_{pt}X_i^{kl})$ , and the nor-

malizing condition  $\sum_i X_i^p = 1$ , for the number operators  $X_i^p = X_i^{pl} X_i^{lp}$  of  $|p\rangle$ -state on site  $i$ . Such a representation of electronic operators is typical for models of strongly correlated electron systems such as superconducting cuprates [29], manganites [30], cobaltites [31], and optical lattices [32, 33]. Using the root vector notations introduced in [34] allows us to obtain a much more compact form of the Hamiltonian in the configurational representation. In our case, the number of subbands is relatively small, and we use bulky but simple notations which make the projection procedure used below more transparent.

In the configurational representation, the model Hamiltonian takes the form  $H = H_0 + T$ . Here,  $H_0$  sums the “atomic limit” terms, and the translational part can be decomposed as  $T = \sum_{n,m} T_{nm}$ , where  $n, m$  serve for numbering the “atomic” states. Terms  $T_{nn}$  of the Hamiltonian form the energy subbands, and terms  $T_{nm}$  describe the hybridization of these subbands. Different hopping integrals correspond to transitions in (or between) the different subbands. The subbands of higher-energy processes appear to be narrower due to the correlated hopping of electrons. The relative positions and the overlapping of subbands depends on the relations between the energy parameters. At the integer values of electron concentration ( $n = 1, 2, 3, 4, 5$ ) in the system, the metal-insulator transition is possible. In the partial case of the band filling  $n = 1$ , strong Coulomb correlation, and strong Hund’s coupling (the parameter  $U - 3J_H$  is much greater than the bandwidth, see estimations in [21, 22]), the states with three and more electrons on the same site are excluded. Then the influence of the correlated hopping can be described by three different hopping integrals. The bare band hopping integral  $t_{ij}$  is renormalized with regard for the band narrowing caused by the concentration-dependent correlated hopping as  $t_{ij}(n) = t_{ij}(1 - \tau_1 n)$ . This hopping integral characterizes the lower Hubbard subband. The parameter  $\tau_1$  is usually neglected, but it is of basic importance for a consistent description of correlation effects in narrow band systems (see [19, 20] for a detailed discussion). The hopping integral for the upper Hubbard subband is  $\tilde{t}_{ij}(n) = t_{ij}(n) + 2t'_{ij}$ , and  $\bar{t}_{ij}(n) = t_{ij}(n) + t'_{ij}$  describes a hybridization of the lower and upper Hubbard subbands. In what follows, only the case  $n = 1$  is considered; so, we omit the explicit notation of concentration dependence. Then the Hamiltonian in the  $X$ -operator representation [27] has the form

$$H = H_0 + \sum_{\lambda=\alpha,\beta,\gamma} \left( H_b^{(\lambda)} + H_h^{(\lambda)} \right), \quad (8)$$

$$\begin{aligned} H_0 &= -\mu \sum_{i\sigma} \left( X_i^{\sigma 00} + X_i^{0\sigma 0} + X_i^{00\sigma} + \right. \\ &+ 2 \left( X_i^{\sigma\sigma 0} + X_i^{\sigma 0\sigma} + X_i^{0\sigma\sigma} \right) \left. + \right. \\ &+ (U - 3J_H) \sum_{i\sigma} \left( X_i^{\sigma\sigma 0} + X_i^{\sigma 0\sigma} + X_i^{0\sigma\sigma} \right), \\ H_b^{(\alpha)} &= \sum_{ij\sigma} \left( t_{ij} X_i^{\sigma 00,000} X_j^{000,\sigma 00} + \right. \\ &+ \tilde{t}_{ij} X_i^{\sigma\sigma 0,0\sigma 0} X_j^{0\sigma 0,\sigma\sigma 0} + \tilde{t}_{ij} X_i^{\sigma 0\sigma,00\sigma} X_j^{00\sigma,\sigma 0\sigma} + \\ &+ \tilde{t}_{ij} X_i^{\sigma\sigma 0,0\sigma 0} X_j^{00\sigma,\sigma 0\sigma} + \tilde{t}_{ij} X_i^{\sigma 0\sigma,00\sigma} X_j^{0\sigma 0,\sigma\sigma 0} \left. \right), \\ H_h^{(\alpha)} &= \sum_{ij\sigma} \bar{t}_{ij} \left( X_i^{\sigma 00,000} X_j^{0\sigma 0,\sigma\sigma 0} + X_i^{\sigma\sigma 0,0\sigma 0} X_j^{000,\sigma 00} + \right. \\ &+ X_i^{\sigma 00,000} X_j^{00\sigma,\sigma 0\sigma} + X_i^{\sigma 0\sigma,00\sigma} X_j^{000,\sigma 00} \left. \right), \\ H_b^{(\beta)} &= \sum_{ij\sigma} \left( t_{ij} X_i^{0\sigma 0,000} X_j^{000,0\sigma 0} + \right. \\ &+ \tilde{t}_{ij} X_i^{\sigma\sigma 0,\sigma 00} X_j^{\sigma 00,\sigma\sigma 0} + \tilde{t}_{ij} X_i^{0\sigma\sigma,00\sigma} X_j^{00\sigma,0\sigma\sigma} - \\ &- \tilde{t}_{ij} X_i^{\sigma\sigma 0,\sigma 00} X_j^{00\sigma,0\sigma\sigma} - \tilde{t}_{ij} X_i^{0\sigma\sigma,00\sigma} X_j^{\sigma 00,\sigma\sigma 0} \left. \right), \\ H_h^{(\beta)} &= \sum_{ij\sigma} \bar{t}_{ij} \left( X_i^{0\sigma 0,000} X_j^{00\sigma,0\sigma\sigma} + X_i^{0\sigma\sigma,00\sigma} X_j^{000,0\sigma 0} - \right. \\ &- X_i^{0\sigma 0,000} X_j^{\sigma 00,\sigma\sigma 0} - X_i^{\sigma\sigma 0,\sigma 00} X_j^{000,0\sigma 0} \left. \right), \\ H_b^{(\gamma)} &= \sum_{ij\sigma} \left( t_{ij} X_i^{00\sigma,000} X_j^{000,00\sigma} + \right. \\ &+ \tilde{t}_{ij} X_i^{\sigma 0\sigma,\sigma 00} X_j^{\sigma 00,\sigma 0\sigma} - \tilde{t}_{ij} X_i^{0\sigma\sigma,0\sigma 0} X_j^{0\sigma 0,0\sigma\sigma} + \\ &+ \tilde{t}_{ij} X_i^{\sigma 0\sigma,\sigma 00} X_j^{0\sigma 0,0\sigma\sigma} + \tilde{t}_{ij} X_i^{0\sigma\sigma,0\sigma 0} X_j^{\sigma 00,\sigma 0\sigma} \left. \right), \\ H_h^{(\gamma)} &= -\sum_{ij\sigma} \bar{t}_{ij} \left( X_i^{00\sigma,000} X_j^{\sigma 00,\sigma 0\sigma} + X_i^{\sigma 0\sigma,\sigma 00} X_j^{000,00\sigma} + \right. \\ &+ X_i^{00\sigma,000} X_j^{0\sigma 0,0\sigma\sigma} + X_i^{0\sigma\sigma,0\sigma 0} X_j^{000,00\sigma} \left. \right). \end{aligned}$$

The technique of Green functions allows us to calculate the energy spectrum within the model, which corresponds to the electronic subsystem of  $A_xC_{60}$  in the case of the electron concentration  $n = 1$ . One can rewrite the single-particle Green function  $\langle\langle a_{i\lambda\sigma}^+ | a_{j\lambda\sigma}^+ \rangle\rangle$  on the basis of the relation between electronic operators and Hubbard's  $X$ -operators:

$$\begin{aligned} a_{p\alpha\uparrow} &= X_p^{000,\uparrow 00} + X_p^{0\uparrow 0,\uparrow 0\uparrow} + X_p^{00\uparrow,\uparrow 0\uparrow} \equiv \\ &\equiv X_p^{000,\uparrow 00} + Y_p, \end{aligned} \quad (9)$$

where the operator  $Y_p$  describes the transition processes between doubly occupied Hund's state and singly occupied state. The processes involving the other types of doubly occupied states, empty states, and states with three or more electrons are improbable due to the energy scaling.

In this way, we obtain the following expression for the single-electron Green function

$$\begin{aligned} \langle\langle a_{p\alpha\uparrow} | a_{p'\alpha\uparrow}^+ \rangle\rangle &= \langle\langle X_p^{000,\uparrow 00} | X_{p'}^{\uparrow 00,000} \rangle\rangle + \\ &+ \langle\langle X_p^{000,\uparrow 00} | Y_{p'}^+ \rangle\rangle + \langle\langle Y_p | X_{p'}^{000,\uparrow 00} \rangle\rangle + \langle\langle Y_p | Y_{p'}^+ \rangle\rangle. \end{aligned} \quad (10)$$

The equation of motion for the Green function  $\langle\langle X_p^{000,\uparrow 00} | X_{p'}^{\uparrow 00,000} \rangle\rangle$  has the form

$$\begin{aligned} (E + \mu) \langle\langle X_p^{000,\uparrow 00} | X_{p'}^{\uparrow 00,000} \rangle\rangle &= \\ = \delta_{pp'} \frac{X_p^{000} + X_p^{\uparrow 00}}{2\pi} + \langle\langle [X_p^{000,\uparrow 00}; \sum_{\lambda} H_b^{(\lambda)}] | X_{p'}^{\uparrow 00,000} \rangle\rangle \\ &+ \langle\langle [X_p^{000,\uparrow 00}; \sum_{\lambda} H_h^{(\lambda)}] | X_{p'}^{\uparrow 00,000} \rangle\rangle, \end{aligned} \quad (11)$$

and the equation of motion for the Green function  $\langle\langle Y_p | X_{p'}^{000,\uparrow 00} \rangle\rangle$  looks as

$$\begin{aligned} (E + \mu - U + 3J_H) \langle\langle Y_p | X_{p'}^{000,\uparrow 00} \rangle\rangle &= \\ = \langle\langle [Y_p; \sum_{\lambda} H_b^{(\lambda)}] | X_{p'}^{\uparrow 00,000} \rangle\rangle + \langle\langle [Y_p; \sum_{\lambda} H_h^{(\lambda)}] | X_{p'}^{\uparrow 00,000} \rangle\rangle. \end{aligned} \quad (12)$$

To obtain the closed system of equations for the Green functions  $\langle\langle X_p^{000,\uparrow 00} | X_{p'}^{\uparrow 00,000} \rangle\rangle$  and  $\langle\langle Y_p | X_{p'}^{000,\uparrow 00} \rangle\rangle$ , we use the projection procedure similar to that in [28]:

$$[X_p^{000,\uparrow 00}; \sum_{\lambda} H_b^{(\lambda)}] = \sum_i \varepsilon_{pi}^b X_i^{000,\uparrow 00};$$

$$[X_p^{000,\uparrow 00}; \sum_{\lambda} H_h^{(\lambda)}] = \sum_i \varepsilon_{pi}^h Y_i;$$

$$[Y_p; \sum_{\lambda} H_b^{(\lambda)}] = \sum_i \tilde{\varepsilon}_{pi}^b Y_i;$$

$$[Y_p; \sum_{\lambda} H_h^{(\lambda)}] = \sum_i \tilde{\varepsilon}_{pi}^h X_i^{000,\uparrow 00}. \quad (13)$$

Performing the Fourier transformation, we obtain the Green function in the form:

$$\begin{aligned} \langle\langle X_i^{000,\uparrow 00} | X_j^{\uparrow 00,000} \rangle\rangle_{\mathbf{k}} &= \frac{X^{000} + X^{\uparrow 00}}{2\pi} \times \\ &\times \frac{E + \mu - U + 3J_H - \tilde{\varepsilon}^b(\mathbf{k})}{(E - E_1(\mathbf{k}))(E - E_2(\mathbf{k}))}, \end{aligned} \quad (14)$$

where the quasiparticle energy spectrum

$$\begin{aligned} E_{1,2}(\mathbf{k}) &= -\mu + \frac{U - 3J_H}{2} + \frac{\varepsilon^b(\mathbf{k}) + \tilde{\varepsilon}^b(\mathbf{k})}{2} \mp \\ &\mp \frac{1}{2} \sqrt{(U - 3J_H - \varepsilon^b(\mathbf{k}) + \tilde{\varepsilon}^b(\mathbf{k}))^2 + 4\varepsilon^h(\mathbf{k})\tilde{\varepsilon}^h(\mathbf{k})}. \end{aligned} \quad (15)$$

In the absence of orbital order, the energy spectrum for  $\beta$  and  $\gamma$  electrons is the same as that for  $\alpha$  electrons.

The non-operator coefficients  $\varepsilon^b(\mathbf{k})$ ,  $\tilde{\varepsilon}^b(\mathbf{k})$ ,  $\varepsilon^h(\mathbf{k})$ ,  $\tilde{\varepsilon}^h(\mathbf{k})$  can be obtained by the anticommutation of Eq.(13) with the basis operators  $X_i^{000,\uparrow 00}$  and  $Y_i^+$  and the following replacement of operators by  $c$ -numbers (see in this connection [19]). We have

$$\begin{aligned} \varepsilon_{\mathbf{k}}^b &= \frac{1}{C_1} \left[ t_{\mathbf{k}} (\langle X_p^{000} (X_{p'}^{000} + X_{p'}^{\uparrow 00}) \rangle) + \right. \\ &+ \langle X_p^{\uparrow 00} (X_{p'}^{000} + X_{p'}^{\uparrow 00}) \rangle + \langle X_p^{\downarrow 00,\uparrow 00} X_{p'}^{\uparrow 00,\downarrow 00} \rangle + \\ &\langle X_p^{0\uparrow 0,\uparrow 00} X_{p'}^{\uparrow 00,0\uparrow 0} \rangle + \langle X_p^{0\downarrow 0,\uparrow 00} X_{p'}^{\uparrow 00,0\downarrow 0} \rangle + \\ &+ \langle X_p^{00\uparrow,\uparrow 00} X_{p'}^{\uparrow 00,00\uparrow} \rangle + \langle X_p^{00\downarrow,\uparrow 00} X_{p'}^{\uparrow 00,00\downarrow} \rangle \\ &\left. - \tilde{t}_{\mathbf{k}} (\langle X_p^{\uparrow 00,000} X_{p'}^{000,\uparrow 00} \rangle + \langle X_p^{\uparrow 00,000} X_{p'}^{000,\uparrow 00} \rangle) \right], \\ \varepsilon_{\mathbf{k}}^h &= \frac{1}{C_2} \tilde{t}_{\mathbf{k}} \left[ \langle (X_p^{000} + X_p^{\uparrow 00}) \times \right. \end{aligned}$$

$$\begin{aligned}
 & \times (X_{p'}^{0\uparrow 0} + X_{p'}^{00\uparrow} + X_{p'}^{\uparrow 0} + X_{p'}^{\uparrow 0\uparrow}) + \\
 & + \langle X_p^{0\uparrow 0, \uparrow 00} X_{p'}^{\uparrow 0, 0\uparrow\uparrow} \rangle + \langle X_p^{\uparrow 0, 000} X_p^{000, \uparrow 0\uparrow} \rangle - \\
 & - \langle X_p^{0\uparrow 0, \uparrow 00} X_p^{\uparrow 00, 0\uparrow 0} \rangle - \langle X_p^{00\uparrow, \uparrow 00} X_{p'}^{\uparrow 00, 00\uparrow} \rangle + \\
 & + \langle X_p^{\uparrow 0\uparrow, 000} X_p^{000, \uparrow 0\uparrow} \rangle - \langle X_p^{00\uparrow, \uparrow 00} X_{p'}^{\uparrow 0\uparrow, 0\uparrow\uparrow} \rangle, \\
 \tilde{\varepsilon}_{\mathbf{k}}^b = & -\frac{t_{\mathbf{k}}}{C_2} \left[ \langle X_{p'}^{\uparrow 0, 000} X_p^{000, \uparrow 0\uparrow} \rangle + \langle X_{p'}^{\uparrow 0\uparrow, 000} X_p^{000, \uparrow 0\uparrow} \rangle \right] + \\
 & + \frac{\tilde{t}_{\mathbf{k}}}{C_2} \left[ \langle X_p^{0\uparrow 0} + X_p^{\uparrow 0} + X_p^{00\uparrow} + X_p^{\uparrow 0\uparrow} \rangle \times \right. \\
 & \times \langle X_{p'}^{0\uparrow 0} + X_{p'}^{\uparrow 0} + X_{p'}^{00\uparrow} + X_{p'}^{\uparrow 0\uparrow} \rangle + \\
 & + \langle X_p^{0\uparrow 0, \uparrow 00} X_{p'}^{\uparrow 00, 0\uparrow 0} \rangle + \langle X_p^{0\uparrow\uparrow, \uparrow 0\uparrow} X_{p'}^{\uparrow 0\uparrow, 0\uparrow\uparrow} \rangle - \\
 & - \langle X_p^{0\uparrow 0, \uparrow 00} X_{p'}^{\uparrow 0\uparrow, 0\uparrow\uparrow} \rangle - \langle X_p^{0\uparrow\uparrow, \uparrow 0\uparrow} X_{p'}^{\uparrow 00, 0\uparrow 0} \rangle + \\
 & + \langle X_p^{00\uparrow, \uparrow 00} X_{p'}^{\uparrow 00, 00\uparrow} \rangle + \langle X_p^{0\uparrow\uparrow, \uparrow 0\uparrow} X_{p'}^{\uparrow 0\uparrow, 0\uparrow\uparrow} \rangle + \\
 & \left. + \langle X_p^{00\uparrow, \uparrow 00} X_{p'}^{\uparrow 0\uparrow, 0\uparrow\uparrow} \rangle + \langle X_p^{0\uparrow\uparrow, \uparrow 0\uparrow} X_{p'}^{\uparrow 00, 00\uparrow} \rangle \right], \\
 \tilde{\varepsilon}_{\mathbf{k}}^h = & -\frac{\bar{t}_{\mathbf{k}}}{C_1} \left[ \langle (X_{p'}^{000} + X_{p'}^{\uparrow 00}) \times \right. \\
 & \times \langle X_p^{\uparrow 0} + X_p^{\uparrow 0\uparrow} + X_p^{0\uparrow 0} + X_p^{00\uparrow} \rangle + \\
 & + \langle X_p^{0\uparrow\uparrow, \uparrow 0\uparrow} X_{p'}^{\uparrow 00, 0\uparrow 0} \rangle - \langle X_p^{0\uparrow 0, \uparrow 00} X_{p'}^{\uparrow 00, 0\uparrow 0} \rangle + \\
 & + \langle X_p^{\uparrow 0\uparrow, 000} X_p^{000, \uparrow 0\uparrow} \rangle + \langle X_p^{00\uparrow, \uparrow 00} X_{p'}^{\uparrow 00, 00\uparrow} \rangle - \\
 & \left. - \langle X_p^{\uparrow 0\uparrow, 000} X_p^{000, \uparrow 0\uparrow} \rangle + \langle X_p^{0\uparrow\uparrow, \uparrow 0\uparrow} X_{p'}^{\uparrow 00, 00\uparrow} \rangle \right],
 \end{aligned}$$

where  $C_1 = \langle X_p^{000} + X_p^{\uparrow 00} \rangle$ ,  $C_2 = \langle X_p^{0\uparrow 0} + X_p^{00\uparrow} + X_p^{\uparrow 0} + X_p^{\uparrow 0\uparrow} \rangle$ . It is worth to note that, in a partial case of the band filling  $n = 1$  and the strong Coulomb correlation,

we work with the reduced Hilbert space of electronic states, so  $C_1 + C_2 = 1$ .

Let us denote the concentration of empty lattice sites by  $e$  and the concentration of sites singly occupied by electrons with spin  $\sigma$  in the orbital state  $\lambda$  by  $s_{\lambda\sigma}$ . Moreover, the concentrations of Hund's doublons, Hubbard doublons, and non-Hund doublons are denoted by  $d_\sigma$ ,  $d_2$ , and  $\tilde{d}$ , respectively. In the paramagnetic state,  $s_{\lambda\sigma} = s$  and  $d_\sigma = d$ . In the case of strong Hund's coupling, the high-energy doublon configurations are excluded,  $d_2 = \tilde{d} = 0$ . We can use the completeness condition for the  $X$ -operator set to have constraint  $e + 6s + 6d = 1$ , which, under the condition  $e = 6d$ , leads to the relation

$$s = \frac{1 - 12d}{6}. \quad (16)$$

Finally in the paramagnetic case at  $n = 1$ , we obtain

$$\varepsilon^b = \frac{216d^2 - 12d + 1}{24d + 1} t_{\mathbf{k}} + \frac{72d^2}{24d + 1} \tilde{t}_{\mathbf{k}}; \quad (17)$$

$$\varepsilon^h = \bar{t}_{\mathbf{k}} \frac{7d - 12d^2}{1 - 6d}, \quad (18)$$

$$\tilde{\varepsilon}^b = t_{\mathbf{k}} \frac{36d^2}{1 - 6d} + \frac{\tilde{t}_{\mathbf{k}}}{2(1 - 6d)}, \quad (19)$$

$$\tilde{\varepsilon}^h = t_{\mathbf{k}} \frac{24d + 1 - 216d^2}{3(24d + 1)}. \quad (20)$$

In this way, the energy spectrum depends on the concentration of doublons  $d$  (through the dependence of non-operator coefficients). The doublon concentration is determined by the condition

$$6d = \frac{1}{2N} \sum_{\mathbf{k}} \left( \frac{A_e(\mathbf{k})}{\exp(\frac{E_1(\mathbf{k})}{kT}) + 1} + \frac{B_e(\mathbf{k})}{\exp(\frac{E_2(\mathbf{k})}{kT}) + 1} \right), \quad (21)$$

where

$$A_e(\mathbf{k}) = \frac{1}{2} \left( 1 + \frac{U - 3J_H + \tilde{\varepsilon}^b - \varepsilon^b}{\sqrt{(U - 3J_H - \varepsilon^b + \tilde{\varepsilon}^b)^2 + 4\varepsilon^h \tilde{\varepsilon}^h}} \right),$$

$$B_e(\mathbf{k}) = 1 - A_e(\mathbf{k}). \quad (22)$$

Using the model rectangular density of states at zero temperature, we obtain

$$6d = \frac{1}{4w} \int_{-w}^w \frac{A_e(\varepsilon) \Theta(-E_1(\varepsilon))}{E - E_1(\varepsilon)} d\varepsilon +$$

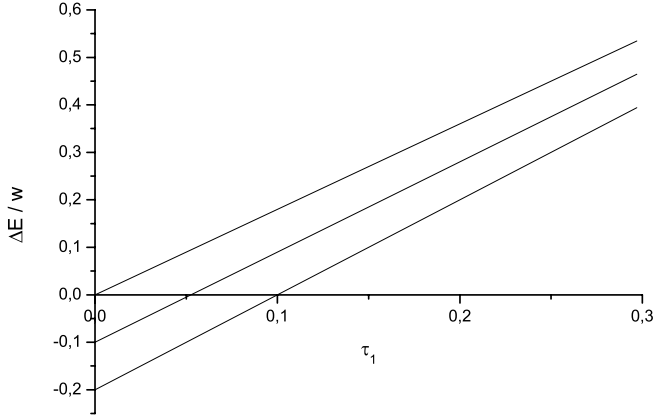


Fig. 2. Energy gap versus the correlated hopping parameter  $\tau_1$ . The values of  $\tau$  are 0; 0.05; 0.1 (starting from the lower curve). The Coulomb interaction parameter  $\frac{U-3J_H}{w} = 2$

$$+ \frac{1}{4w} \int_{-w}^w \frac{B_e(\varepsilon)\Theta(-E_2(\varepsilon))}{E - E_2(\varepsilon)} d\varepsilon, \quad (23)$$

where  $\Theta(-E(\varepsilon))$  is the Heaviside theta-function. Solving this equation numerically, we obtain the doublon concentration as a function of the model parameters. To study the metal-insulator transition (MIT) [35–37], we apply the gap criterion

$$\Delta E = E_2(-w) - E_1(w) = 0. \quad (24)$$

At the point of MIT, the concentrations of polar states (holes and doublons) are equal to zero. Thus, for the non-operators coefficients, we have  $\varepsilon^b = t_{\mathbf{k}}$ ,  $\varepsilon^h = 0$ ,  $\tilde{\varepsilon}^b = \frac{t_{\mathbf{k}}}{2}$ ,  $\tilde{\varepsilon}^h = \frac{t_{\mathbf{k}}}{3}$ . The energy gap satisfies the equation

$$\Delta E = U - 3J_H - \tilde{w} - w. \quad (25)$$

Here,  $w = z|t|(1 - \tau_1)$  and  $\tilde{w} = z|t|(1 - \tau_1)(1 - 2\tau)$  are the half-bandwidths of the lower and upper subbands, respectively,  $z$  is the number of nearest neighbors for a site,  $|t|$  is the magnitude of the bare nearest-neighbor hopping integral,  $\tau_1$  and  $\tau = \frac{t'_{ij}}{|t_{ij}|}$  are the correlated hopping parameters. From relation (25), we obtain that the critical value of intrasite Coulomb interaction parameter equals the sum of the half-bandwidths of quasiparticle subbands.

The analysis of expression (25) allows us to explain the differences of electrical characteristics (of the insulator or metallic state) depending on the correlated hopping strength (see Figs. 2 and 3).

One can see from Fig. 2 that the correlated hopping influences substantially the electrical characteristics of

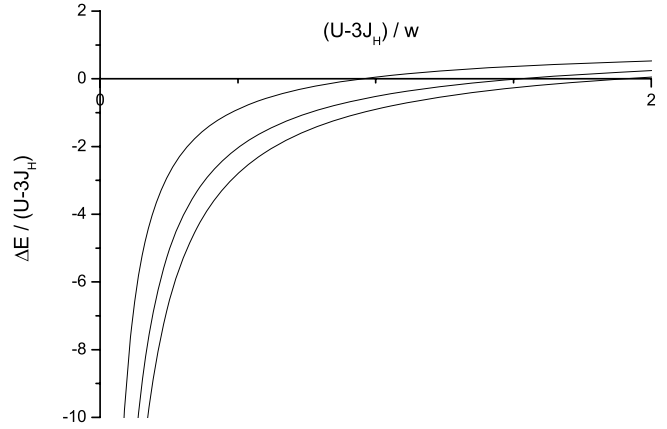


Fig. 3. Energy gap versus the Coulomb interaction parameter at the electron concentration  $n = 1$ . The correlated hopping parameters are  $\tau_1 = 0.05$ ,  $\tau = 0; 0.2; 0.5$  (starting from the lower curve)

the narrow band material with three-fold orbital degeneracy of the energy levels. Both the filling of the sites involved into the hopping processes (through the first-type correlated hopping) and the neighbor sites (through the second-type correlated hopping) can lead to the appearance of a gap in the energy spectrum and the stabilization of the insulator state. However, the energy gap is opened at a relatively large increase of correlated hopping parameters, which can not be achieved in the compound by a change of external conditions only. Such critical increase of the parameters  $\tau_1$  and  $\tau$  can be realized at the doping. A distinct picture is observed at a change of the intrasite Coulomb interaction parameter. Under an increase of  $(U - 3J_H)/w$  over the critical value (dependent on the correlated hopping strength), the energy gap occurs, and the metal-insulator transition takes place (see Fig. 3). The critical value in the partial case of the model where the quasiparticle subbands have the same widths (in the absence of the correlated hopping) is  $(U - 3J_H)/w = 2$ , which corresponds to the result of works [28, 38] based on the non-degenerated Hubbard model.

### 3. Conclusions

Within a version of the triply orbitally degenerate model of the electronic subsystem of a doped fulleride compound considered above, not only the on-site Coulomb correlations but also additional interactions of basic importance, namely the correlated hopping, can be introduced and analyzed. The use of Hubbard representation of  $X$ -operators appears useful to omit the parts of the



Hilbert space, which are irrelevant at a particular band filling. The ground-state metal-insulator transition in the triply degenerate model of partially-filled doped fulleride band takes place at moderate values of the correlation parameter. In this case, this parameter is a combination of the on-site Coulomb repulsion energy, Hund's rule coupling, and electron hopping parameters. The correlated hopping of electrons leads to a further localization of current carriers. The influence of the correlated hopping is substantial and makes the estimation of the model parameters from the available spectroscopic data ambiguous. The problem can be resolved by the additional spectroscopic experiments with the use of the external pressure. In this case, the reasonable estimates could be obtained using the fact that, as distinct from the on-site parameters, the correlated hopping parameters must be pressure-dependent. The metal-insulator transition described above can be realized [39, 40] in doped fulleride compounds under the external pressure.

1. A.V. Eletskii and B.M. Smirnov, *Phys. Usp.* **38**, 935 (1995).
2. N. Manini and E. Tosatti, *cond-mat/0602134*.
3. S. Saito and A. Oshiyama, *Phys. Rev. Lett.* **66**, 2637 (1991).
4. Y. Achiba, *Chem. Lett.* **20**, 1233 (1991).
5. P. Heyney, *Phys. Rev. Lett.* **66**, 2911 (1991).
6. J.M. Hawkins, *Acc. Chem. Res.* **25**, 150 (1992).
7. R.M. Fleming, *Nature* **352**, 787 (1991).
8. K. Holczer, O. Klein, and S.M. Huang, *Science* **252**, 1154 (1991).
9. B.V. Reddy, S.N. Khanna, and P. Jena, *Science* **258**, 1640 (1992).
10. D.S. Bethune, G. Meijer, W.C. Tang, and H.J. Rosen, *Chem. Phys. Lett.* **179**, 219 (1990).
11. M.N. Regeiro, *Nature* **354**, 289 (1991).
12. R.O. Zaitsev, *JETP Lett.* **57**, 130 (1993).
13. R.O. Zaitsev, *Pis'ma Zh. Eksp. Teor. Fiz.* **94**, 224 (2011).
14. O. Gunnarsson, E. Koch, and R.M. Martin, *Phys. Rev. B* **56**, 1146 (1997).
15. D.M. Poirier *et al.*, *Phys. Rev. B* **47**, 9870 (1993).
16. S. Satpathy *et al.*, *Phys. Rev. B* **46**, 1773 (1992).
17. Jian Ping Lu, *Phys. Rev. B* **49**, 5687 (1994).
18. A.L. Fetter and J.D. Walecka, *Quantum Theory of Many-Particle Systems* (McGraw-Hill, New York, 1971).
19. L. Didukh, *Acta Phys. Polon. B* **31**, 3097 (2000).
20. L. Didukh, Yu. Skorenkyy, Yu. Dovhopyaty, and V.Hankevych, *Phys. Rev. B* **61**, 7893 (2000).
21. M.R. Pederson and A.A. Quong, *Phys. Rev. B* **46**, 13584 (1992).
22. V.P. Antropov, O. Gunnarsson, and O. Jepsen, *Phys. Rev. B* **46**, 13647 (1992).
23. R.L. Hettich, R.N. Compton and R.H. Ritchie, *Phys. Rev. Lett.* **67**, 1242 (1991).
24. R.W. Lof, M.A. van Veenendaal, B. Koopmans, H.T. Jonkman, and G.A. Sawatzky, *Phys. Rev. Lett.* **68**, 3924 (1992).
25. P.A. Bruhwiler, A.J. Maxwell, A. Nilsson, N. Martensson, and O. Gunnarsson, *Phys. Rev. B* **48**, 18296 (1993).
26. R.L. Martin and J.P. Ritchie, *Phys. Rev. B* **48**, 4845 (1993).
27. J. Hubbard, *Proc. Roy. Soc. A* **285**, 542 (1965).
28. L. Didukh, *J. Phys. Stud.*, **1**, 241 (1997).
29. S.G. Ovchinnikov, *Phys. Rev. B* **49**, 9891 (1994).
30. V.A. Gavrichkov, S.G. Ovchinnikov, I.A. Nekrasov, and Z.V. Pchelkina, *Zh. Eksp. Teor. Fiz.* **139**, 983 (2011).
31. S.G. Ovchinnikov, Yu.S. Orlov, I.A. Nekrasov, and Z.V. Pchelkina, *JETP* **112**, 140 (2011).
32. I.V. Stasyuk, T.S. Mysakovych, *Condens. Matter Phys.* **12**, 539 (2009).
33. I.V. Stasyuk, T.S. Mysakovych, and V.O. Krasnov, *Condens. Matter Phys.* **13**, 13003 (2010).
34. R.O. Zaitsev, *Sov. Phys. JETP* **43**, 574 (1976).
35. N.F. Mott, *Metal-Insulator Transitions* (Taylor & Francis, London, 1990).
36. *Metal-Insulator Transitions*, edited by P.P. Edwards and C.N.R. Rao (Taylor & Francis, London, 1995).
37. F. Gebhard, *The Mott Metal-Insulator Transition: Models and Methods* (Springer, Berlin, 1997).
38. L. Didukh, *Phys. Stat. Sol.(b)* **206**, R5 (1998).
39. L. Degiorgi, *Adv. in Physics* **47**, 207 (1998).
40. H. Sakamoto *et al.*, *Synth. Met.* **121**, 1103 (2001).

Received 20.05.11

МОТТ-ГАВБАРДІВСЬКА ЛОКАЛІЗАЦІЯ В МОДЕЛІ  
ЕЛЕКТРОННОЇ ПІДСИСТЕМИ ЛЕГОВАНОГО  
ФУЛЛЕРИДУ

*Ю. Довгоп'ятий, Л. Дідух, О. Крамар, Ю. Скоренький,  
Ю. Дрогобицький*

## Резюме

Досліджено конфігураційне представлення мікроскопічної моделі електронної підсистеми легованого фулериду з урахуванням трикратного орбітального виродження електронних станів. З використанням методу функцій Гріна розраховано енергетичний спектр моделі при заповненні зони  $n = 1$ , що відповідає сполукам  $AC_{60}$ . Обговорено можливий кореляційно індукований перехід діелектрик-метал у рамках даної моделі.

МОТТ-ХАВБАРДОВСКАЯ ЛОКАЛИЗАЦИЯ В МОДЕЛИ  
ЭЛЕКТРОННОЙ ПОДСИСТЕМЫ ЛЕГИРОВАННОГО  
ФУЛЛЕРИДА

*Ю. Довгоп'ятий, Л. Дідух, О. Крамар, Ю. Скоренький,  
Ю. Дрогобицький*

## Резюме

Исследовано конфигурационное представление микроскопической модели электронной подсистемы легированного фуллерида с учетом трехкратного орбитального вырождения электронных состояний. С использованием метода функций Грина рассчитан энергетический спектр модели при заполнении зоны  $n = 1$ , что соответствует соединениям  $AC_{60}$ . Обсужден возможный корреляционно индуцированный переход диелектрик-металл в рамках данной модели.